World Scientific
www.worldscientific.com

Raman spectroscopy for detection of imatinib in plasma: A proof of concept

Sanhita Rath[*,¶], Aditi Sahu[†,¶], Vikram Gota[*], P. G. Martínez-Torres[‡],
J. L. Pichardo-Molina[∥] and C. Murali Krishna[†,§]

[*]Department of Clinical Pharmacology, ACTREC
Tata Memorial Center, Kharghar
Navi Mumbai 410210 India

[†]Chilakapati Lab, ACTREC, Tata Memorial Center
Kharghar, Navi Mumbai 410210 India

[‡]Instituto de Física y Matemáticas
Universidad Michoacana de San Nicolás de Hidalgo
Edificio C-3, Ciudad Universitaria
CP. 58040 Morelia, Michoacán, México

[∥]Centro de Investigaciones en Óptica AC
C.P. 37 #150, León Gto., Mexico
[§]mchilakapati@actrec.gov.in
[§]pittu1043@gmail.com

Imatinib is the standard first line treatment for chronic myeloid leukemia (CML). Owing to dose-related toxicities of Imatinib such as neutropenia, there is scope for treatment optimization through therapeutic drug monitoring (TDM). Trough concentration of $1\,\mu g/mL$ is considered the therapeutic threshhold. Existing methods for the detection of Imatinib in plasma are limited by long read out time and expensive instrumentation. Hence, Raman spectroscopy was explored as a rapid and objective tool for monitoring Imatinib concentration. Three approaches: conventional Raman spectroscopy (CRS), Drop coating deposition Raman (DCDR) spectroscopy and surface-enhanced Raman spectroscopy (SERS) were employed to detect the required trough concentration of $1\,\mu g/mL$ and above. Detection of therapeutically relevant concentrations ($1\,\mu g/mL$) using SERS and suitable nanoparticle substrates has been demonstrated. Prospectively, rigorous validation using clinical samples is necessary to confirm the utility of this approach in routine clinical usage.

Keywords: Therapeutic drug monitoring; Raman spectroscopy; Imatinib; SERS; DCDR; chronic myeloid leukemia.

[§]Corresponding author.
[¶]Equally contributed.

1. Introduction

Tyrosine kinase inhibitors revolutionized the concept of well-tolerated cancer therapy with the introduction of Imatinib for the first line treatment of chronic phase chronic myeloid leukemia (CML). Imatinib inhibits ABL and the BCR-ABL fusion protein, c-KIT, and the platelet-derived growth factor receptor (PDGF-R).[1] It is also used for the treatment of Philadelphia positive acute lymphoblastic leukemia (ALL), gastrointestinal stromal tumors (GIST) and some cases of dermatofibrosarcoma protuberans. The standard dose used in adults is 400 mg once daily, whereas children with Philadelphia chromosome-positive leukemia receive a standard daily dose of $340 \, mg/m^2$.[2] Trough Imatinib plasma concentrations above $1 \, \mu g/mL$ are associated with complete cytogenetic and major molecular responses to standard dose (400 mg once daily) in chronic myeloid leukemia.[3] Variations in drug disposition, especially plasma clearance (CL), may result in excessive toxicity or suboptimal anticancer efficacy. The main toxicities of Imatinib are frequently dose-related. For instance, Neutropenia correlates with the area under the concentration time curve (AUC) of Imatinib.[4] Owing to the exposure effect relationship, Imatinib is an ideal candidate for therapeutic drug monitoring (TDM),[5] that would allow for optimization of dose to achieve improved molecular response in CML.[6] Liquid chromatography mass spectrometry (LC-MS) and high performance liquid chromatography (HPLC) are widely used and clinically practiced methods for the detection of Imatinib levels.[7]

In view of long sample preparation time and non-availability of instrumentation in standard hospital settings, there is a need to develop an alternative rapid yet accurate method for the determination of plasma Imatinib concentrations. Raman spectroscopic (RS) studies in biomedicine, pharmaceutics and homeland security applications (for detection of biomarkers, chemicals, explosives) have already been well documented.[8–10] Variants of RS such as drop coating deposition Raman (DCDR) and surface-enhanced Raman spectroscopy (SERS) are known to be sensitive and can facilitate detection up to single molecule level. With DCDR, a type of non-enhanced Raman spectroscopy, applications such as analyzing changes in the relative protein concentrations of aqueous tertiary protein mixtures and determination of albumin glycation have been reported.[11–13] SERS is a well known and time-tested technique for ultrasensitive detection, analysis and imaging at single molecule level.[14,15] This paper introduces the utility of Raman spectroscopy as a prospective tool for rapid monitoring of patients treated with Imatinib, at the therapeutic concentration of $1 \, \mu g/mL$ and above.

2. Materials and Methods

2.1. *Sample preparation*

Different concentrations of Imatinib ranging from $5 \, mg/mL$ to $1 \, \mu g/mL$ were spiked in ultrapure water (Milli-Q systems, Millipore Corporation and referred to as "milli-q" in the manuscript) and pooled plasma (obtained from blood banks). A series of stock solutions were prepared and serially diluted for their corresponding analysis. To ensure repeatability and reproducibility, each concentration was analyzed in triplicates and the experiment was repeated three times on different days.

2.2. *Raman spectroscopy*

2.2.1. *Instrumentation*

Spectra were recorded using fiberoptic Raman microprobe (Horiba-Jobin-Yvon, France), as described elsewhere.[16] This Raman system consists of laser (785 nm, Process Instruments) as an excitation source and HE-785 spectrograph (Horiba-Jobin-Yvon, France) coupled with CCD (Synapse, Horiba-Jobin-Yvon) as dispersion and detection elements, respectively. Optical filtering of unwanted noise, including Rayleigh signals, is accomplished through "Superhead", the other component of the system. Optical fibers were employed to carry the incident light from the excitation source to the sample and also to collect the Raman scattered light from the sample to the detection system. Raman microprobe was assembled by coupling a 40X (NA: 0.65) microscope objective (Nikon, Japan) to the superhead.

2.2.2. *Experimental approaches*

All spiked samples were subjected to conventional RS by placing approximately $10 \, \mu L$ of sample on a CaF_2 window. The spectra were recorded randomly from multiple points on each drop using the setup described above.

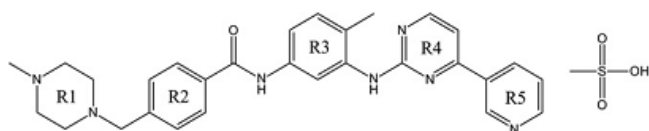In case of DCDR, a volume of $10 \, \mu L$ (sample spiked with drug) was deposited on CaF_2 substrates

Table 1.   Peak assignments for Imatinib.

Imatinib saturated solution (cm^{-1})	Assignment
782	R3 (methylbenzene ring)
996	R4 (Aminopyrimidine ring) + S = O (mesylate salt)
1048	R1 (N-methyl piperazine ring)
1324	R1 (N-methyl piperazine ring)
1424	R5 (Pyridine ring)
1615	R2

and allowed to dry for approximately 40 min in a Fume hood. The dried drop was subjected to RS. Spectra were acquired from one end of the drop (periphery) to the other (vertical direction). This was repeated by spanning the drop across the horizontal direction to investigate the presence of Imatinib in the dried drop.

SERS studies were carried out by depositing concave gold nanoparticles on glass substrates coated with aluminum foil substrates. Concave nanocubes were synthesized with slight modifications in the method reported by Zhang *et al.*[17] In a typical synthesis, seeds were prepared in the following way: 260 μL of HAuCl$_4$ (10 mM) were added to a 10 mL of cetyltrimethylammonium chloride (CTAC) solution (0.1 M), to initiate the seeds growth, 700 μL of ice-cold freshly prepared NaHB$_4$ solution (10 mM) was
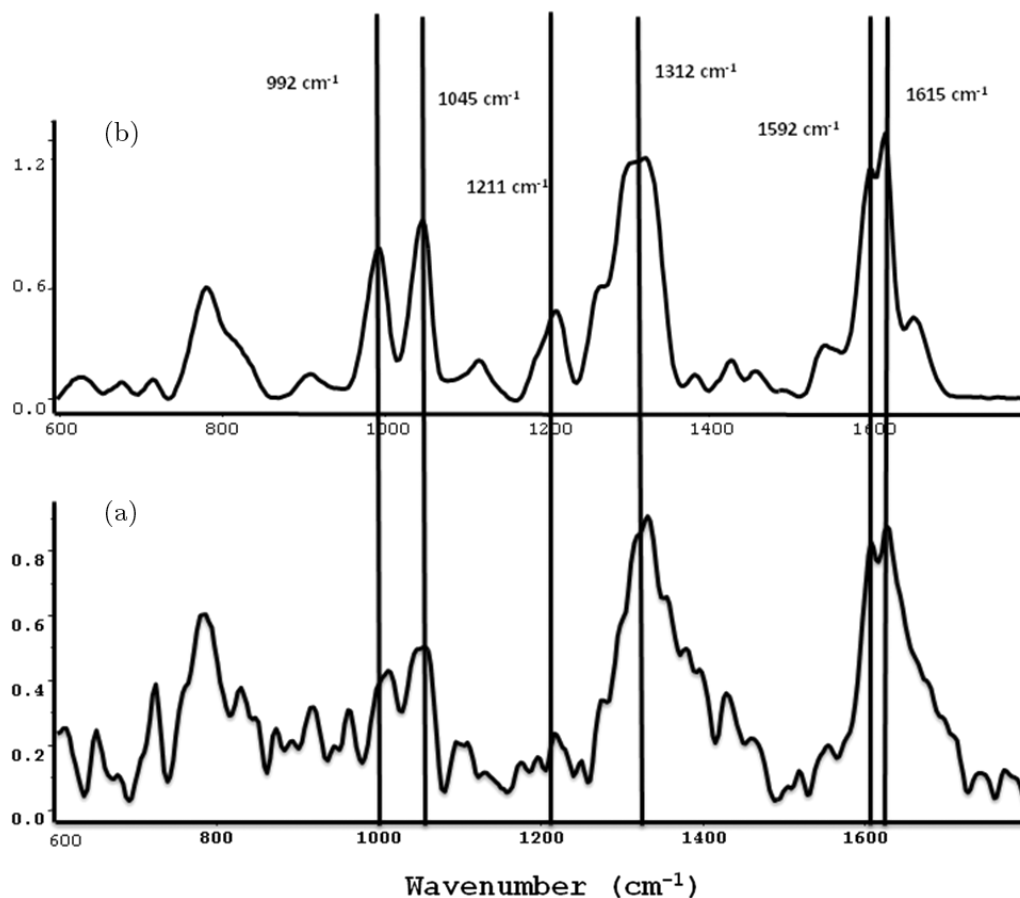

Fig. 1.   Representative spectra for conventional Raman approach in drug spiked milli-q. Spectra were acquired from Imatinib spiked milli-q and representative spectra for 5 and 1 mg/mL are shown in the figure, (a) Lowest concentration: 1 mg/mL, (b) Highest concentration: 5 mg/mL.

added under continuous magnetic stirring and left standing for 2 min and finally left undisturbed for 2 h. For concave nanocubes, growth solution was prepared by consecutively adding: 10 mL of CTAC (0.1 M), 500 μL of HAuCl$_4$ (10 mM), 50 μL of AgNO$_3$ (10 mM), 200 μL of HCl (1 M), 125 μL of ascorbic acid (0.1 M). 50 μL of seeds solution diluted 1:100 were added to the growth solution to initiate the growth of the nanoparticles. The nanoparticles were harvested from the surfactants and other media components by centrifugation at 3500 rpm for 30 min. This washing step was repeated 3 times to obtain purified nanoparticles with minimal media components.[18] SERS substrates were prepared by dropping

20 μL of purified nanoparticles on the surface of cleaned aluminum foil. After the nanoparticles dried, spiked water and plasma solutions were dropped onto the SERS substrate and the corresponding Raman spectra were acquired at random points of the sample.

Spectral acquisition parameters of laser power — 30 mW, acquisition time — 15 s, average — 4 were kept constant for all the measurements (CRS, DCDR and SERS). The laser spot size at the sample was $\sim$ 5–10 μm. About 10 spectra were recorded from different areas of the drop, in case of CRS and SERS. For DCDR, $\sim$ 15 spectra were acquired from one end of the drop to the other, both horizontally and vertically as previously stated. The
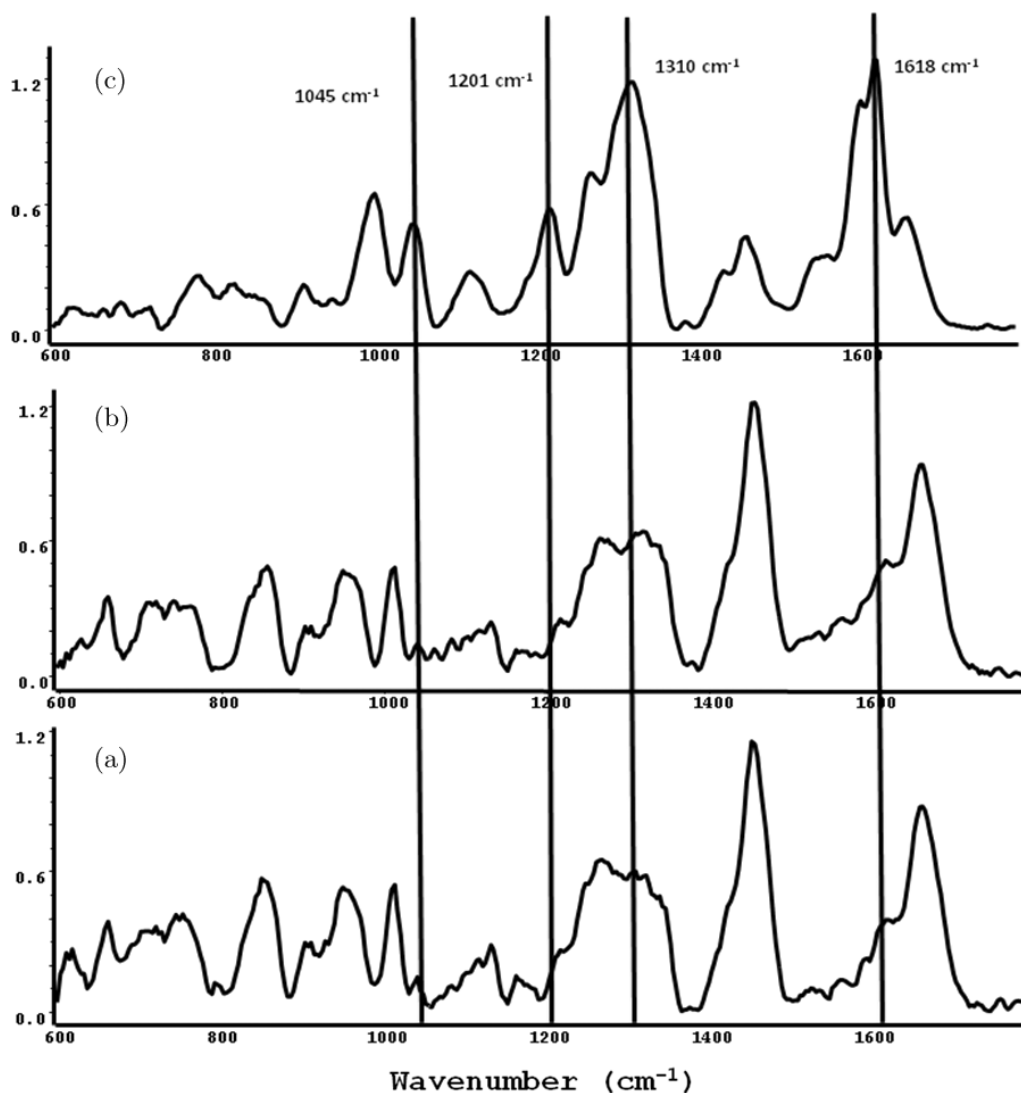

Fig. 2.   Representative spectra for DCDR approach in drug spiked and blank plasma. DCDR approach was explored to achieve lower detection limit for Imatinib. Spectra were acquired from dried drop of Imatinib spiked plasma for concentrations 2, 1, 0.1 mg/mL and blank plasma. Imatinib-specific signals could be observed till 0.1 mg/mL; (a) blank plasma, (b) Lowest concentration: 0.1 mg/mL, (c) Intermediate concentration: 1 mg/mL, (d) Highest concentration: 2 mg/mL.

representative spectrum from each class has been shown in the manuscript.

2.2.3. *Spectra pre-processing*

Raman spectra were corrected for charged coupled device (CCD) response with a National Institute of Science and Technology (NIST) certified Standard Reference Material 2241 (SRM 2241) followed by the subtraction of background signals from optical elements and substrate. Spectra were interpolated in $600–1800\,\mathrm{cm}^{-1}$ region. Details of the spectral pre-processing are mentioned elsewhere.[16] Average spectra were computed from these background-subtracted and interpolated spectra. The typical spectra were baseline-corrected by fitting a fifth-order polynomial function using LabSpec 4.18 (Horiba Jobin Yvon, France). These baseline-corrected, smoothed (Savitzky–Golay, 3) and vector-normalized spectra were analyzed for detecting Raman signals attributable to Imatinib and computing difference spectra.

3. Results and Discussion

While RS has been used for various other applications discussed earlier, its use for detection of drugs like Imatinib in biological matrices has not been explored. Existing methods such as HPLC and
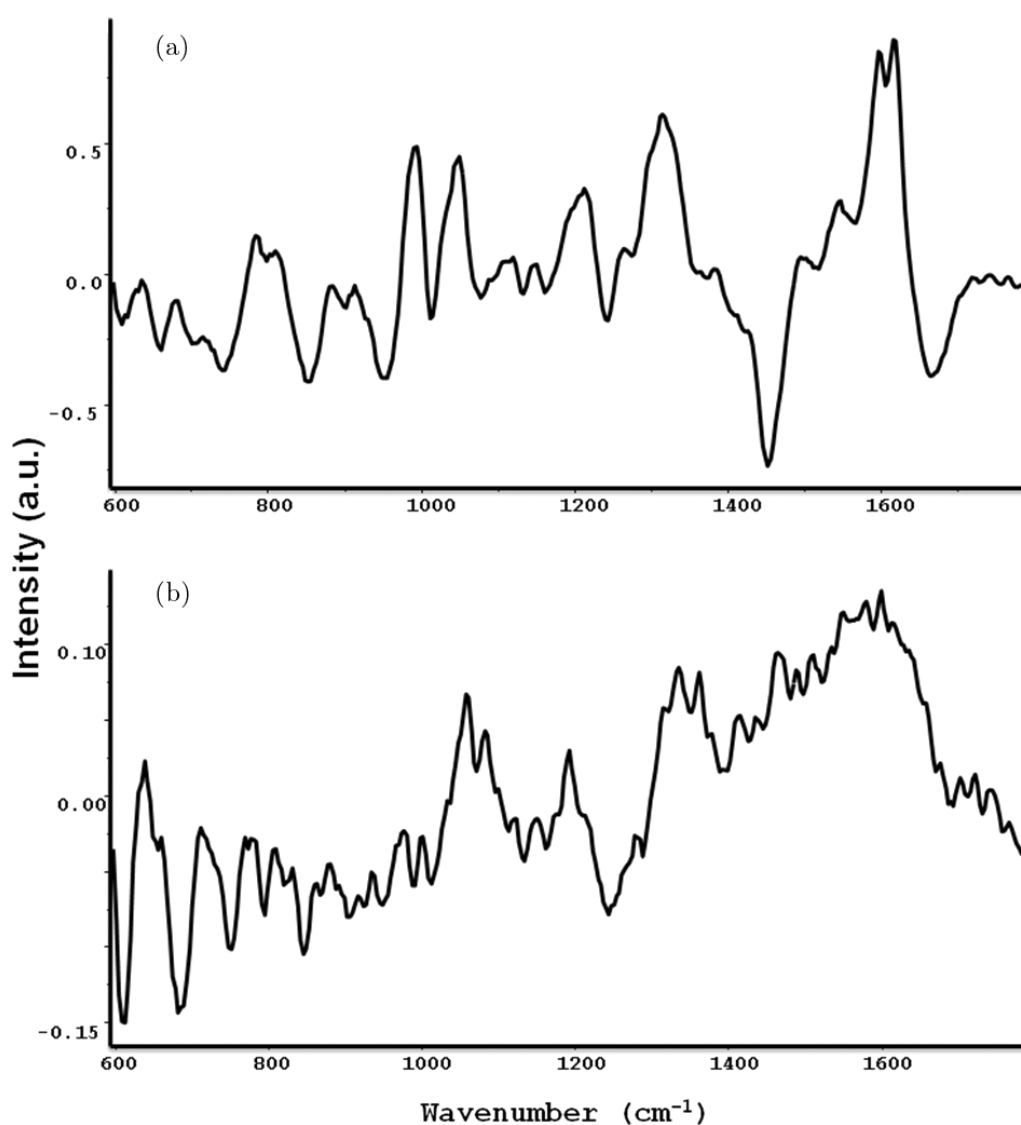

Fig. 3.   Difference spectra for DCDR approach (a) Highest concentration (2 mg) — blank plasma, (b) Lowest concentration (0.1 mg) — blank plasma.

LC-MS being used for the purpose are resource-consuming and labor intensive. This prompted us to explore an alternative method for therapeutic monitoring of Imatinib. The RS method described here for the detection of Imatinib in plasma is the first to be reported so far.

The potential of Raman spectroscopy as therapeutic tool for detection of Imatinib was explored using three approaches: conventional Raman spectroscopy (CRS), DCDR and SERS. The chemical name for imatinib is 4-[(4-methyl-1-piperazinyl) methyl]-N-[4-methyl-3-[[4-(3-pyridinyl)-2-pyrimidinyl]amino]-phenyl]benzamide methanesulfonate. For a pure/saturated Imatinib solution, spectra were acquired using the same experimental setup and bands were observed at positions 782, 996, 1048, 1310, 1424, 1600 and 1623 cm^{-1}. These

bands can be attributed to the following structural components in Imatinib: 996 cm^{-1} band can be attributed to R4 (aminopyrimidine ring) and v(S=O) (mesylate salt), 1048 cm^{-1} is assigned to R1 (N-methyl piperazine ring) and R5 (pyridine ring), 1310 cm^{-1} is attributed to R1 and R2 (benzamide ring). 1424 cm^{-1} can be assigned to R4 and R5 while R2 vibrations are associated with 1615 cm^{-1}. Spectral assignments were made based on the available literature, and are also tabulated in Table 1.[19,20] The same standard bands were used to identify Imatinib in the spiked samples.

3.1. *Conventional Raman spectroscopy*

The feasibility of detecting Imatinib was first evaluated using CRS in drug-spiked milli-q. The baseline corrected spectra acquired using CRS are shown in
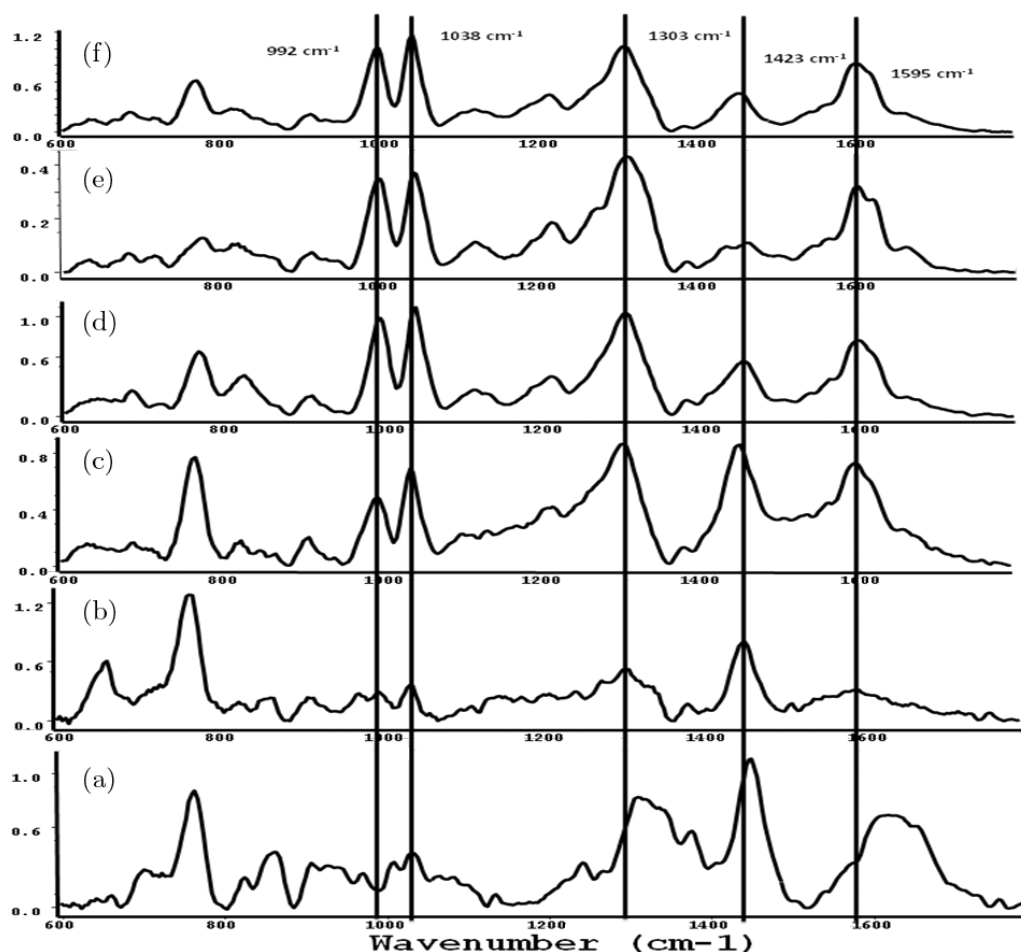

Fig. 4.   Representative spectra for SERS approach in drug-spiked milli-q. SERS approach to achieve therapeutically relevant concentrations was first investigated in milli-q. Concentrations ranging from 1–0.001 mg/mL were spiked in milli-q and deposited on suitable nanoparticle substrates. Imatinib-specific signals could also be detected in the lowest concentration. (a) Blank nanoparticles, (b) Lowest concentration: 0.001 mg/mL (1 μg/mL), (c) Concentration: 0.01 mg/mL, (d) Concentration: 0.1 mg/mL, (e) Concentration: 0.5 mg/mL, (f) Highest concentration: 1 mg/mL.

Figs. 1(a) and 1(b). Major Raman bands indicating the presence of Imatinib in the highest concentration (5 mg/mL), were observed at 782, 992, 1045, 1211, 1312, 1598 and 1615 cm^{-1} [Fig. 1(b)].[19,20] The lowest limit of detection of Imatinib using CRS was found to be 1 mg/mL, where minor bands attributable to Imatinib were observed at 992, 1045 and 1211 cm^{-1} [Fig. 1(a)]. The presence of Imatinib in 1 mg/mL was confirmed using difference spectra computed by subtracting blank milli-q from 1 mg/mL concentration (data not shown). Positive bands at 990, 1044, 1321, 1598 and 1618 cm^{-1} verify the detection of Imatinib for this concentration. With a detection limit way above the desired therapeutic threshold of 1 μg/mL, this approach proved to be inefficient for use from a clinical perspective.

3.2. *DCDR*

In order to improve sensitivity and evaluate the detection of Imatinib in human plasma, the technique of DCDR was employed. For these experiments,

concentrations starting from 2 mg/mL up till 0.1 mg/mL of Imatinib spiked in plasma were employed. The baseline corrected spectra are shown in Figs. 2(a)–2(c). As seen in Fig. 2(a), major Raman bands for blank plasma were observed at 1660, 1450, 1265, 1128 and 1008 cm^{-1} attributed to Amide I (protein), CH$_2$ stretch (lipid and protein), Amide III (protein), C–N stretching (protein) and Phe, respectively along with bands at 946, 1114, 1306, 1320 and 1618 cm^{-1}. For the highest concentration of drug-spiked plasma (2 mg/mL), major bands were observed at 996, 1045, 1114, 1214, 1262, 1313, 1457, 1598, 1618 and 1657 cm^{-1} [Fig. 2(c)]. The Imatinib reference spectra is suggestive that bands at 996, 1045, 1214 1313, 1598 and 1618 cm^{-1} may be indicative of Imatinib. Imatinib-related bands were also observed in the successive lower concentrations, down to 0.1 mg/mL, where bands at 1211, 1313 and 1618 cm^{-1} [Fig. 2(b)] can be attributed to Imatinib. To confirm the presence of Imatinib, difference spectra were computed from the highest and lowest concentration by subtracting blank plasma spectra.
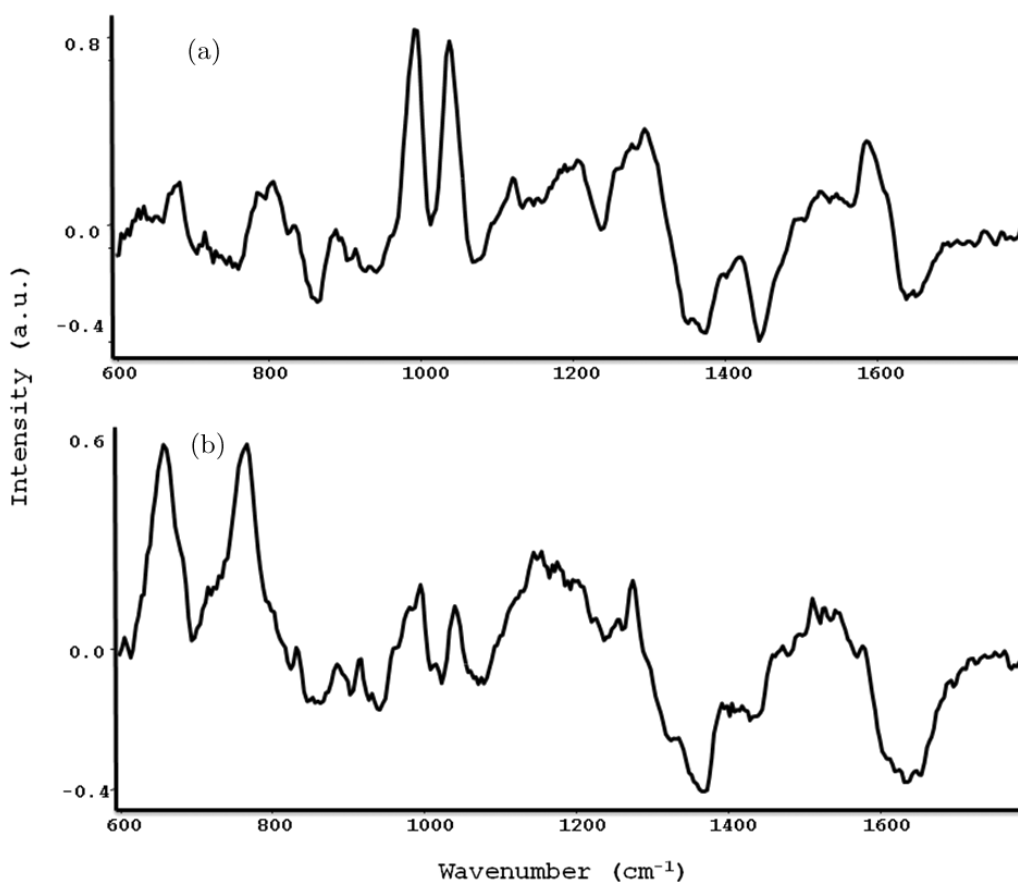

Fig. 5. Difference spectra for SERS approach. (a) Highest concentration (1 mg) — blank nanoparticle, (b) Lowest concentration (1 μg) — blank nanoparticles.

As seen in the Fig. 3(a), positive bands at 998, 1049, 1211, 1311, 1595 and 1615 cm^{-1} indicate the presence of Imatinib in the difference spectrum (2 mg — blank) for a concentration of 2 mg/mL. Negative bands at 1240, 1270, 1450 and 1660 cm^{-1} correspond to contributions from plasma, and are not drug features. In the lowest concentration difference spectrum (0.1 mg — blank), two minor bands at 1595 and 1615 cm^{-1} reflect the presence of Imatinib. Thus, DCDR enabled the detection of concentration as low as 0.1 mg/mL, but it failed to achieve detection of therapeutically relevant concentration i.e., 1 μg/mL.

3.3. *SERS*

SERS was consequently explored for detecting Imatinib at clinically relevant concentrations, owing to its sensitivity up to the single molecule

level. Feasibility SERS experiments were initially carried out in milli-q for drug concentrations of 1, 0.5, 0.1, 0.01 and 0.001 mg/mL, baseline corrected spectra are shown in Fig. 4. In case of drug-spiked water, highly intense bands were observed in higher concentrations (1, 0.5 and 0.1 mg/mL) at 992, 1034, 1303 and 1595 cm^{-1} due to enhancements because of drug–metal interactions [Figs. 4(d)–4(f)]. Other bands observed at 763 and 1207 cm^{-1} could also be attributed to Imatinib. In the lowest concentration of 0.001 mg/mL (1 μg/mL), imatinib-related bands were observed at 995, 1034 and 1303 cm^{-1} [Fig. 4(b)]. Difference spectra were computed to confirm this limit of detection. Blank nanoparticle spectrum was subtracted from the highest (1 mg/mL) and lowest concentrations (1 μg/mL), as shown in Fig. 5. Positive bands at 990, 1034, 1294 and 1585 cm^{-1} in
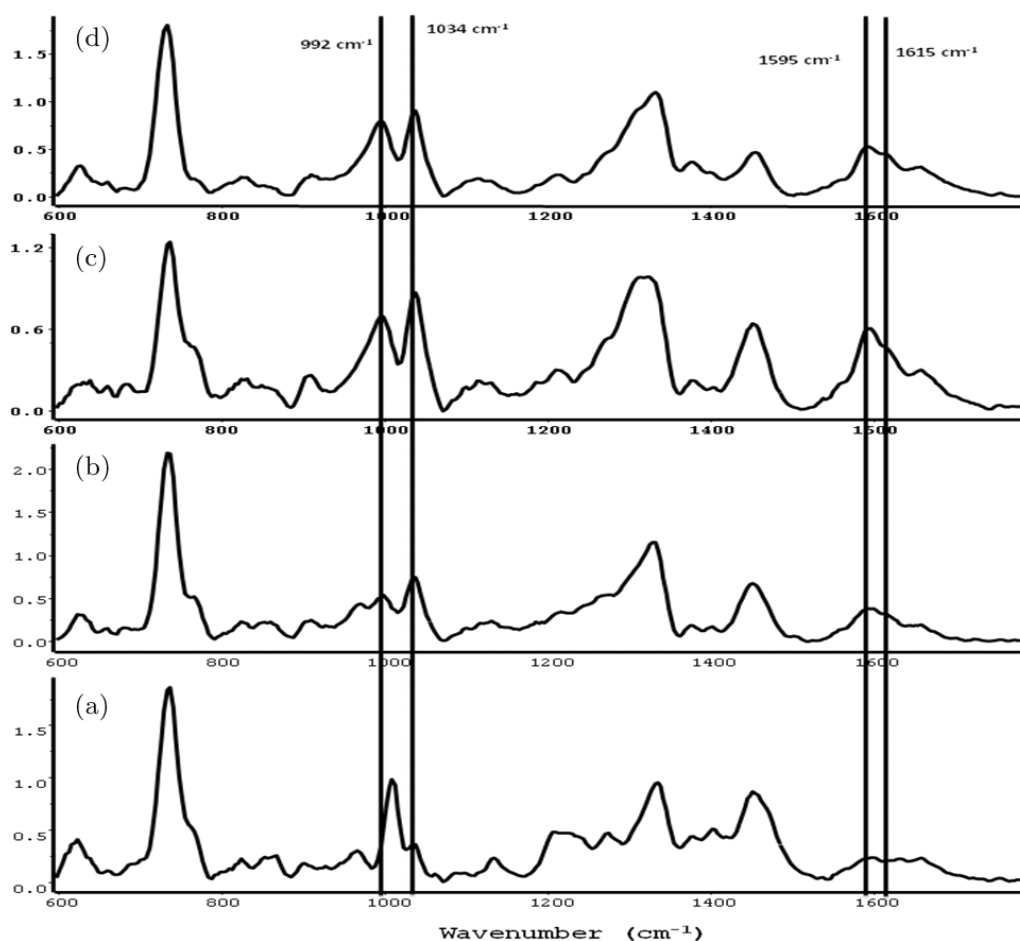

Fig. 6. Representative spectra for SERS approach in drug-spiked plasma. SERS approach to achieve therapeutically relevant concentrations was then investigated in drug-spiked plasma. Concentrations ranging from 0.1–0.001 mg/mL were spiked in plasma and deposited on suitable nanoparticle substrates. Imatinib-specific signals could also be detected in the lowest concentration. (a) Blank plasma, (b) Lowest concentration: 0.001 mg/mL (1 μg/mL), (c) Concentration: 0.005 mg/mL, (d) Highest concentration: 0.1 mg/mL.

Fig. 5(a) can be attributed to Imatinib. In the lowest concentration difference spectrum, major positive bands were observed at 653, 763, 992, 1038 and 1152 cm^{-1}. Of these, bands at 992 and 1034 cm^{-1} may be indicative of Imatinib detection at this concentration (1 μg/mL). Further, the feasibility of detecting Imatinib in drug-spiked plasma was evaluated (Fig. 6). The concentrations 0.1, 0.005 and 0.001 mg/mL were spiked in plasma. The highest concentration showed bands at 992, 1034, 1592 and 1615 cm^{-1} [Fig. 6(d)], while minor bands could also be observed at similar band positions in the 1 μg/mL concentration [Fig. 6(b)] with respect to blank plasma [Fig. 6(a)]. A difference spectrum was calculated by subtracting blank plasma from the highest (0.1 mg/mL) and lowest concentration (1 μg/mL). Major positive bands for the highest concentration difference spectrum was seen at 719, 985, 1034, 1107,

1303, 1592 and 1611 cm^{-1}, of which 985, 1034, 1303, 1592 and 1618 cm^{-1} can be attributed to Imatinib [Fig. 7(a)]. In the lowest concentration difference spectra, positive bands were observed at 727, 985, 1034, 1114, 1176, 1259, 1296 and 1592 cm^{-1}. Bands at 985, 1034, 1296 and 1592 cm^{-1} can be attributed to Imatinib [Fig. 7(b)]. Thus, the therapeutic detection limits of 1 μg/mL was achieved using both drug-spiked milli-q and plasma. The reproducibility of the approach was confirmed by multiple repetitions of the experiment. Thus, SERS with suitable nanoparticles substrates can lead to peak enhancements that enabled detection at the required therapeutic concentration of 1 μg/mL.

The advantage of using RS-based approach for drug monitoring of Imatinib is the objectivity, rapidity and the minimal sample preparation requirements. As SERS-nanoparticles-based approach can achieve
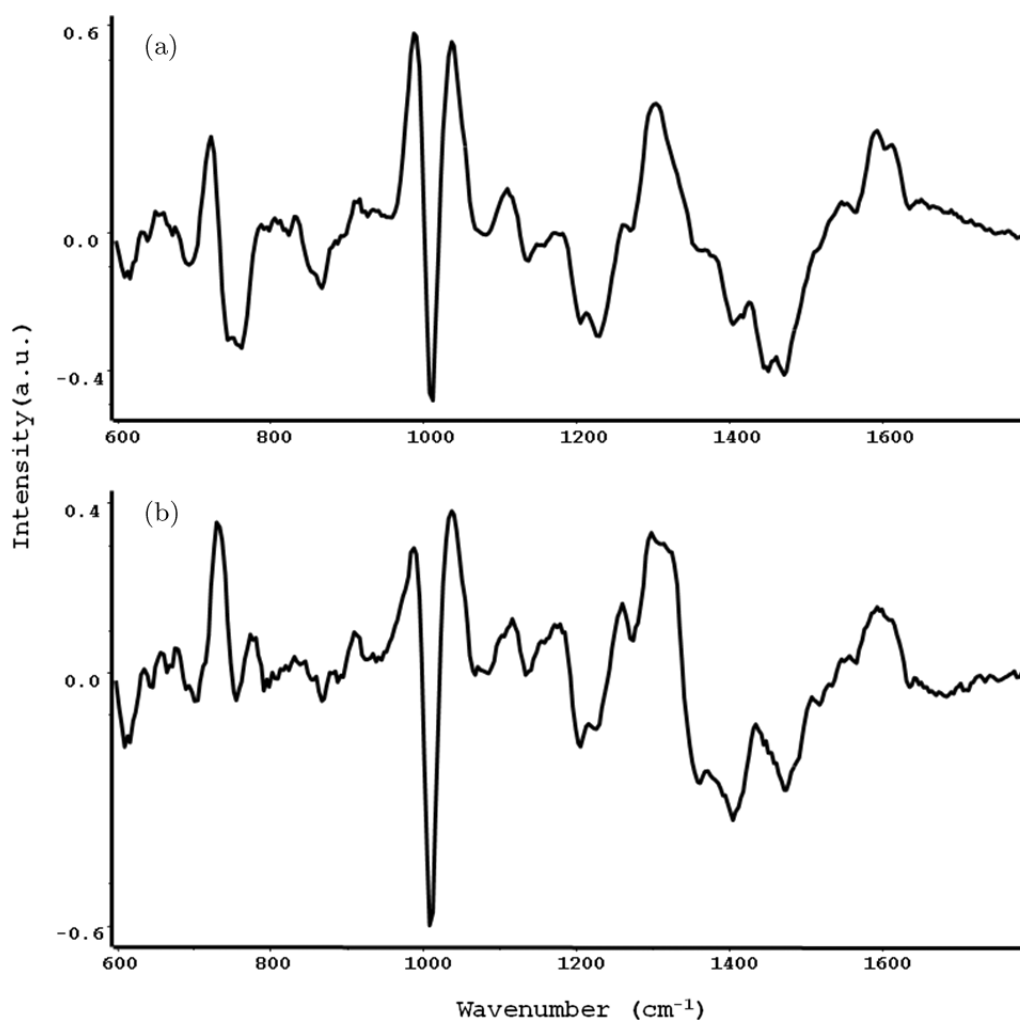

Fig. 7. Difference spectra for SERS approach. (a) Highest concentration (0.1 mg) — blank plasma, (b) Lowest concentration (1 μg) — blank plasma.

the therapeutic detection limits, this approach can be adopted for all future clinical applications. Coating of aluminum substrates with the synthesized nanoparticles is a simple and standardized procedure. Thus, manufacturing ready-to-use substrates on a large scale is not labor intensive. For clinical applications, blood samples from visiting patients can be collected, placed on the already-prepared substrate, and spectral acquisition can be done. The spectra can then be tested against existing standard models of the therapeutically relevant trough and peak concentrations. Drug levels in patients can then be inferred from the result of the test prediction. Thus, an immediate decision on optimal dose can be made. Although, availability of on-site instrumentation at all clinical centers can be a limiting factor, samples can be collected and transported to a centralized facility for Raman analysis, and results can be sought within a few hours of sample receipt.

4. Conclusion

RS, DCDR and SERS approaches were explored for the detection of Imatinib at therapeutic concentration of $1\,\mu g/mL$ and above. Of these, SERS-nanoparticle-based approach can be a more practical and efficient tool for TDM of Imatinib in clinics.

Although HPLC, LC-MS are sensitive as well as precise methods for determination of Imatinib concentration, this study has been designed specifically to detect imatinib at the concentration of $1\,\mu g/mL$ and above. We would like limit the sensitivity to $1\,\mu g/mL$ and above as that is our therapeutic threshold and detection at lower levels may not have clinical utility. Thus, CRS, DCDR and SERS approaches were explored for the detection of Imatinib at therapeutic concentration of $1\,\mu g/mL$ and above. The current study is a proof of concept which introduces a semi-quantitative assay for detection of Imatinib in human plasma. Prospective rigorous validation using clinical samples is required to establish Raman-spectroscopy as a rapid and objective tool for routine clinical usage. This concept can be extended for other drugs which are candidates for TDM.

Acknowledgments

Conflict of Interest

None.

References

1. K. Eechoute, A. Sparreboom, H. Burger, R. M. Franke, G. Schiavon, J. Verweij, W. J. Loos, E. A. Wiemer, R. H. Mathijssen, "Drug transporters and imatinib treatment: Implications for clinical practice," *Clin. Cancer Res.* **17**(3), 406–415 (2011).
2. A. Petain, D. Kattygnarath, J. Azard, E. Chatelut, C. Delbaldo, B. Geoerger, M. Barrois, S. Seronie-Vivien, A. LeCesne, G. Vassal, "Population pharmacokinetics and pharmacogenetics of imatinib in children and adults," *Clin. Cancer Res.* **14**(21), 7102–7109 (2008).
3. S. Picard, K. Titier, G. Etienne, E. Teilhet, D. Ducint, M. A. Bernard, R. Lassalle, G. Marit, J. Reiffers, B. Begaud, N. Moore, M. Molimard, F. X. Mahon, "Trough imatinib plasma levels are associated with both cytogenetic and molecular responses to standard-dose imatinib in chronic myeloid leukemia," *Blood* **109**(8), 3496–3499 (2007).
4. C. Delbaldo, E. Chatelut, M. Ré, A. Deroussent, S. Séronie-Vivien, A. Jambu, P. Berthaud, A. Le Cesne, J.-Y. Blay, G. Vassal, "Pharmacokinetic-Pharmacodynamic relationships of imatinib and its main metabolite in patients with advanced gastro-intestinal stromal tumors," *Clin. Cancer Res.* **12**(20), 6073–6078 (2006).
5. S. Bouchet, B. Royer, C. Le Guellec, K. Titier, "Therapeutic drug monitoring of tyrosine-kinase inhibitors in the treatment of chronic myelogenous leukaemia: Interests and limits," *Therapie* **65**(3), 213–218 (2010).
6. T. P. Hughes, S. Branford, "Monitoring disease response to tyrosine kinase inhibitor therapy in CML," *Hematology* **1**, 477–487 (2009).
7. M. Miura, N. Takahashi, K. Sawada, "Quantitative determination of imatinib in human plasma with high performance liquid chromatography and ultraviolet detection," *J. Chromatogr. Sci.* **49**(5), 412–415 (2011).
8. R. S. Golightly, W. E. Doering, M. J. Natan, "Surface-enhanced Raman spectroscopy and homeland security: A perfect match?," *ACS Nano* **3**(10), 2859–2869 (2009).

9. Q. Tu, C. Chang, "Diagnostic applications of Raman spectroscopy," *Nanomedicine* **8**(5), 545–558 (2012).

10. S. Wartewig, R. H. Neubert, "Pharmaceutical applications of mid-IR and Raman spectroscopy," *Adv. Drug Deliv. Rev.* **57**(8), 1144–1170 (2005).

11. N. C. Dingari, G. L. Horowitz, J. W. Kang, R. R. Dasari, I. Barman, "Raman spectroscopy provides a powerful diagnostic tool for accurate determination of albumin glycation," *PLoS One* **7**(2), e32406 (2012).

12. J. Filik, N. Stone, "Drop coating deposition Raman spectroscopy of protein mixtures," *Analyst* **132**, 544–550 (2007).

13. D. Zhang, Y. Xie, M. F. Mrozek, C. Ortiz, V. J. Davisson, D. Ben-Amotz, "Raman detection of proteomic analytes," *Anal. Chem.* **75**(21), 5703–5709 (2003).

14. K. Kneipp, Y. Wang, H. Kneipp, L. T. Perelman, I. Itzkan, R. R. Dasari, M. S. Feld, "Single molecule detection using surface-enhanced Raman scattering (SERS)," *Phys. Rev. Lett.* **78**, 1667 (1997).

15. W. Xie, S. Schlucker, "Medical applications of surface-enhanced Raman scattering," *Phys. Chem. Chem. Phys.* **15**(15), 5329–5344 (2013).

16. A. Sahu, K. Dalal, S. Naglot, P. Aggarwal, C. M. Krishna, "Serum based diagnosis of asthma using Raman spectroscopy: An early phase pilot study," *PLoS One* **8**(11), e78921 (2013).

17. J. Zhang, M. R. Langille, M. L. Personick, K. Zhang, S. Li, C. A. Mirkin, "Concave cubic gold nanocrystals with high-index facets," *J. Am. Chem. Soc.* **132**, 14012–14014 (2010).

18. Y. P. de León, J. Pichardo-Molina, N. A. Ochoa, "Growth kinetics of concave nanocubes studied by optical coherence tomography," *Plasmonics* **9**, 907–915 (2014).

19. A. Srivastava, B. Joshi, P. Tandon, A. Ayala, A. Bansal, D. Grillo, "Study of polymorphism in imatinib mesylate: A quantum chemical approach using electronic and vibrational spectra," *Spectrochim. Acta A* **103**, 325–332 (2013).

20. F. S. Parker, *Applications of Infrared, Raman and Resonance Raman spectroscopy in Biochemistry*, Plenum Press, New York and London (1983).